COMPARATIVE ANALYSIS OF THE EQUIVALENT COEFFICIENTS OF STIFFNESS AND DAMPING OBTAINED FROM MULTILOBULE AND TILTING PAD JOURNAL BEARING

Gregory Bregion Daniel, gbdaniel@fem.unicamp.br
Katia Lucchesi Cavalca, katia@fem.unicamp.br
Laboratory of Rotating Machinery – Faculty of Mechanical Engineering – Postal Box 6122
University of Campinas - UNICAMP
13083-970, Campinas, SP, Brazil

Abstract. *The dynamic analysis of rotating machines is a complex task, because it involves the analysis of many parameters. Therefore, the investigation of such rotating systems should not only take into account the dynamic behavior of the rotor, but it is also necessary to analyze the interaction between other components of the same system, such as the foundation and the bearings. In rotor-bearing-foundation systems, the vibration transmitted from the rotor through the bearings generates motion in the support structure. The interaction between the support structure and the bearings retransmits the vibration to the rotor. Therefore, the bearings play a very important role in this system by transmitting the forces from the rotor to the foundation. Moreover, from a dynamic analysis point of view, the bearings can greatly influence the stiffness and damping characteristics of the rotor system, affecting the location of the critical speeds and altering the vibration amplitudes. Consequently, the hydrodynamic bearing should be designed according to the operating conditions of the rotating machine, due to its direct influence in the dynamic behavior of the system. For this reason, this work aims to analyze two different classes of hydrodynamic bearings: multilobe journal bearing and tilting pad journal bearing. The multilobe journal bearing is widely used in industries due to its large application (speed and load conditions) and low costs. Conversely, the tilting pad journal bearing has higher costs, but its dynamic behavior is more stable than multilobe journal bearing. The tilting pad journal bearing can be applied in critical operation condition with high rotational speed and high load, and generally, it does not present fluid induced instability (Whirl and Whip). In this work, the equivalent coefficients of stiffness and damping to multilobe journal bearings (cylindrical, elliptical and three-lobe) and tilting pad journal bearing were determined and a comparative analysis is accomplished. The equivalent coefficients are obtained with a spring-damper concept, in order to represent the inherent flexibility and damping of the oil film. The equivalent coefficients of the journal bearings are obtained by computational simulation, solving the Reynolds equation by finite volume method. In this case, the equivalent coefficients are evaluated by the perturbation theory applied to the displacements and velocities of the shaft center inside the bearings. Afterwards, the dynamic behavior of the journal bearings is evaluated and compared in terms of stability, allowing the design foreseen of the application field of the journal bearings.*

Keywords*: hydrodynamic lubrication, multilobe journal bearing; tilting pad journal bearing, stiffness and damping coefficients*

1. INTRODUCTION

The development of the rotating machines is directly related with the reliability and stability of the bearings, because these mechanical components are responsible for supporting the rotor. For that reason, many researches have been accomplished in order to design more stable bearings, as well as to determine the dynamic behavior of the bearings commonly applied in these systems.

The hydrodynamic bearing the most commonly used in rotating machines, because of its high life cycle and high load capacity. The cylindrical hydrodynamic bearing is the mostly applied in the industry, because of the easy manufacturing and, consequently, the low costs involved in it. Conversely, this kind of bearing is significantly susceptive to the fluid induced instability (Whirl and Whip) (Castro and Cavalca, 2008; Gunter, 2005; Bently, 2002). From technical advances in the cylindrical bearings, it was possible to obtain the multilobe hydrodynamic bearing (Elliptical and Three-Lobe bearing). The elliptical and three-lobe bearings present low costs of manufacturing, high load capacity and large application (speed and load conditions). Although the multilobe bearings are also susceptive to fluid induced instability, they can be applied in a significantly larger range of rotational speed than the range obtained from the cylindrical bearings. After the multilobe hydrodynamic bearing, the tilting pad journal bearing was developed. The main advantage of this kind of bearing is the applicability in critical operating conditions with high rotational speed and high load, and generally, it does not present fluid induced instability. Because of that, the tilting pad journal bearings have significant acceptability, although the highest manufacturing costs.

The mathematical model of the hydrodynamic lubrication was presented by Reynolds in 1886 (Reynolds, 1886). The solution of the Reynolds' Equation gives the pressure distribution and, consequently, the hydrodynamic forces actuating in the bearing. Sommerfeld (1904) presented the solution of the Reynolds' Equation for long bearings and Orcvick (1952) presented the solution of the Reynolds' Equation for short bearings. In 1958, Pinkus used the finite differences method to solve the Reynolds' Equation and also to determine the pressure distribution in finite journal bearings (Pinkus, 1958). Moreover, Pinkus obtained the pressure distribution in multilobe hydrodynamic bearings (Pinkus, 1956; Pinkus, 1959).

Lund was the pioneer in the determination of stiffness and damping coefficients in hydrodynamic bearing. In his works, Lund determined the stiffness and damping coefficients in hydrodynamic journal bearing, using the method of perturbations (Lund, 1964; Lund, 1979; Lund, 1987).

The study of stiffness and damping coefficients in journal bearings is a difficult task. Nowadays, many efforts have been directed to obtain the problem solution (Meruane and Pascual, 2008; Wang and Khonsari, 2006).

Recently, Machado and Cavalca (2009) accomplished a comparative analysis between the stiffness and damping coefficients obtained from cylindrical and multilobe hydrodynamic bearings.

Thus, this work aims to compare the stiffness and damping coefficients obtained from cylindrical and multilobe hydrodynamic bearing with those obtained from tilting pad journal bearing. In face of this comparison, it is possible to verify what kind of bearing presents the most stable behavior.

2. METHODOLOGY

The stiffness and damping coefficients in hydrodynamic bearings are evaluated from the hydrodynamic forces actuating in the bearing, obtained from the integration of the pressure distribution in the bearing.

As previously mentioned, the pressure distribution is obtained from the solution of the Reynolds' Equation.

$$\frac{\partial}{\partial x}\left(\frac{h^3}{\mu}\frac{\partial P}{\partial x}\right)+\frac{\partial}{\partial z}\left(\frac{h^3}{\mu}\frac{\partial P}{\partial z}\right)=6\cdot\omega\cdot R\cdot\frac{\partial h}{\partial x}+12\cdot\frac{\partial h}{\partial t} \tag{1}$$

Where $P(x,z)$ is the pressure distribution in the oil film, x e z are the rectangular co-ordinates, μ is the absolute viscosity, R is the radius of the shaft, h is the thickness of the oil film, ω is the rotational speed and t is the time.

The equilibrium position of the shaft inside the bearing is determined from these hydrodynamic forces and the bearing loading.

Afterwards, the stiffness and damping coefficients can be calculated. These coefficients are obtained with a spring-damper concept, in order to represent the inherent flexibility and damping of the oil film. In this case, the coefficients are evaluated by the perturbation theory applied to displacements and velocities of the shaft, when the shaft is in its equilibrium position. The relation between the hydrodynamic forces and the displacements (and velocities) of the shaft center gives the equivalent coefficients.

2.1. Solution of the Reynolds' Equation by Finite Volume Method

Due to the limitations of the analytic solutions, the analysis of hydrodynamic bearings tends to solve the Reynolds' Equation numerically. In this work, the finite volume method was applied as described by Maliska (2004).

To use the finite volume method, it is convenient to reduce the number of variables of the problem applying a dimensionless set. Moreover, from the dimensionless set, it is possible to transform the real domain in a square numerical domain, giving an uniform mesh in both directions. With this purpose, the following dimensionless set is proposed:

$$\bar{x}=\frac{x}{\theta\cdot R} \tag{2}$$

$$\bar{z}=\frac{z}{L} \tag{3}$$

$$\bar{h}=\frac{h}{C_R} \tag{4}$$

$$\bar{\mu}=\frac{\mu}{\mu_0} \tag{5}$$

$$\bar{t}=t\cdot\omega \tag{6}$$

$$\bar{P}=\frac{P}{6\cdot\mu_0\cdot\omega\cdot\left(\frac{R}{C_R}\right)^2} \tag{7}$$

Where: θ is the coverage angle, L is the axial width of the bearing, C_R is the radial clearance and μ_0 is the absolute viscosity of reference.

According to Fig. 1, the geometries of these bearings are different. Thus, θ is different for each kind of bearing. For cylindrical bearings, the value of θ is 2π. However, θ represents the angle of each lobe for elliptical and three-lobe bearings and the angle of each pad for tilting pad journal bearings. Moreover, the thickness of the oil film is also different for each kind of bearing (see Pinkus, 1956; Pinkus, 1958, Pinkus, 1959; Lund, 1964).

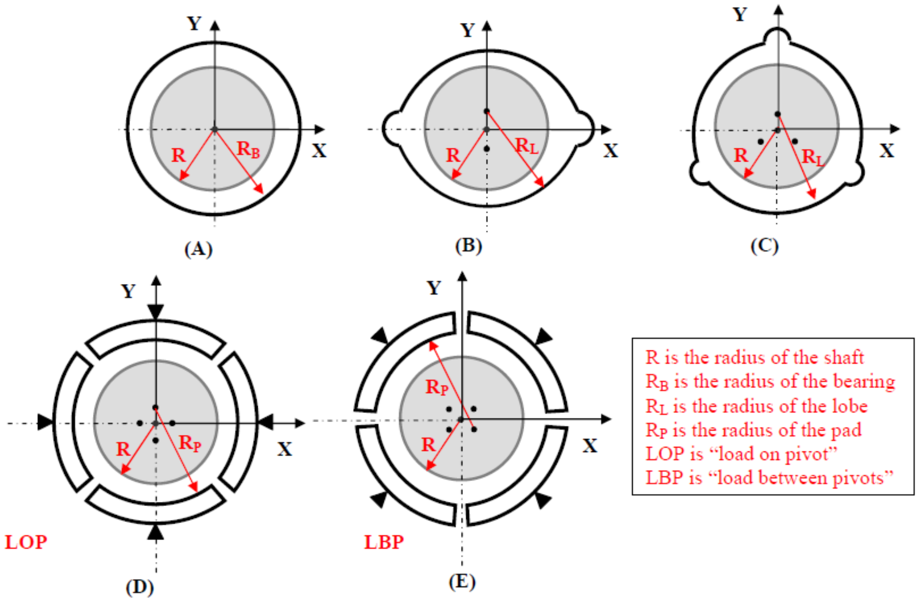

Figure 1. Types of Hydrodynamic Bearing. (A) Cylindrical, (B) Elliptical, (C) Three-Lobe Bearings, (D) Tilting Pad – LOP, (E) Tilting Pad – LBP.

Substituting the dimensionless set in Eq. (1) the dimensionless Reynolds' Equation is:

$$\frac{1}{\theta^2}\cdot\frac{\partial}{\partial\bar{x}}\left(\frac{\bar{h}^3}{\bar{\mu}}\frac{\partial\bar{P}}{\partial\bar{x}}\right)+\left(\frac{L}{R}\right)^2\cdot\frac{\partial}{\partial\bar{z}}\left(\frac{\bar{h}^3}{\bar{\mu}}\frac{\partial\bar{P}}{\partial\bar{z}}\right)=\frac{1}{\theta}\cdot\frac{\partial\bar{h}}{\partial\bar{x}}+2\cdot\frac{\partial\bar{h}}{\partial\bar{t}} \tag{8}$$

According to the mesh in Fig. 2, it is possible to obtain a discretized solution for the Reynolds' Equation:

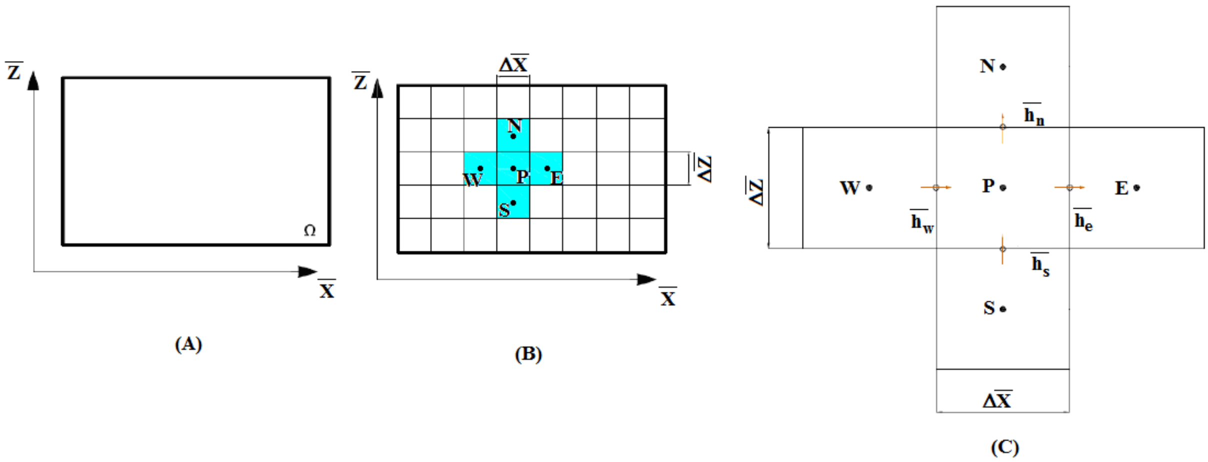

Figure 2. Numerical mesh of the model. (A) Numerical domain, (B) Discretized domain, (C) Representation of the volume P located in the mesh.

Therefore, a mesh of N points results in N algebraic equations, which can be solved by methods of linear systems or iterative methods.

From the pressure distribution, it is possible to evaluate the hydrodynamics forces in the oil film, integrating the pressure distribution, according to the following equations.

$$F_V = \sum_{n=1}^{N} p_n \cos\theta_n(\Delta x)(\Delta z) \tag{9}$$

$$F_H = \sum_{n=1}^{N} p_n \sin\theta_n(\Delta x)(\Delta z) \tag{10}$$

Where F_V and F_H are the hydrodynamic forces in vertical and horizontal directions, respectively.

2.2. Determination of the Stiffness and Damping Coefficients

The equivalent coefficients are obtained applying smalls perturbations of displacements and velocities in the shaft, around the equilibrium position, as described by Lund (1964, 1979, 1987).

The reaction forces are function of the displacement for the shaft (x and y), and of the instantaneous velocities of the shaft ($\dot{x}$ and $\dot{y}$, where "dot" indicates time derivate). Hence, for small variations (Δx , Δy , $\Delta\dot{x}$, $\Delta\dot{y}$) measured from the static equilibrium position (x_0 and y_0), the reaction hydrodynamic forces can be written through the first order Taylor series expansion as:

$$\begin{aligned} F_x &= F_{x0} + K_{xx}\Delta x + K_{xy}\Delta y + B_{xx}\Delta\dot{x} + B_{xy}\Delta\dot{y} \\ F_y &= F_{y0} + K_{yx}\Delta x + K_{yy}\Delta y + B_{yx}\Delta\dot{x} + B_{yy}\Delta\dot{y} \end{aligned} \tag{10}$$

Thus, the coefficients are the partial derivatives evaluated at the equilibrium position (Lund, 1987):

$$K_{xy} = \left(\frac{\partial F_x}{\partial y}\right)_0 \qquad B_{xy} = \left(\frac{\partial F_x}{\partial \dot{y}}\right)_0 \tag{11}$$

and similarly for the remaining coefficients.

In this paper, the coefficients are often computed directly by numerical differentiation by employing a perturbation solution. For the cylindrical, elliptical and three-lobe bearings, the perturbations are applied only in the displacement and velocity of the shaft (Δx , Δy , $\Delta\dot{x}$ and $\Delta\dot{y}$), resulting in eight equivalents coefficients (four stiffness coefficients and four damping coefficients). However, for the tilting pad journal bearings, apart from perturbations applied to the shaft, the perturbations should also be applied in the pads. Thus, there are two additional perturbations ($\Delta\alpha$ and $\Delta\dot{\alpha}$, where α is the tilt angle of the pad) for each pad of the bearing.

According Allaine et al. (1981), each pad results in eighteen coefficients (nine stiffness coefficients and nine damping coefficients) due to the direct and cross coupled coefficients in x, y and α. Thus, these coefficients can be written in a quadratic complex matrix of order N_P+2, where N_P is the number of pads in the bearing. After that, it is possible to reduce this complex matrix to other complex matrix of order 4x4 and, consequently, to obtain the four stiffness coefficients and four damping coefficients of the bearing (Allaine et al., 1981; Russo, 1991). The reduction and determination of the stiffness and damping coefficients depends of the frequency of the perturbations (vibrational frequency). In this work, the vibrational frequency is set at the shaft rotational speed. Thus, the eight reduced coefficients for the tilting pad bearing are designated "synchronously reduced" bearing coefficients.

3. RESULTS

The parameters of the bearings considered in the numerical simulations are presented in the Tab. 1.

Table 1. Parameters of the hydrodynamic bearings considered in the simulations

Radius of the Shaft (R)		0.050 m
Width of the Bearing (L)		0.050 m
Radial Clearance (C_R)		100 µm
Load (W)		400 N
Elliptical bearing	Three-lobe bearing	Tilting pad bearing
Number of lobes (N_L) = 2	Number of lobes (N_L) = 3	Number of pads (N_P) = 4
Axial Grooves (β_A) = 30°	Axial Grooves (β_A) = 30°	Axial Grooves (β_A) = 30°
		Pad thickness (h_S) = 0.0175 m

Regarding to the lubricant fluid, the oil considered in the numerical simulation is the ISO VG 32, whose absolute viscosity is 0.070Pa.s at 30°C.

The mathematical models described in the previous chapter don't considerer the cavitation condition because it is supposed that the bearings are completely filled with oil.

The results of this paper show the stiffness and damping coefficients and the locus of the shaft for cylindrical, elliptical, three-lobe and titling pad journal bearing (LOP-LBP), considering values of preload (m) equal 0, 0.25, 0.5 and 0.75. The rotation speed range considered in the simulations is from 20 RPS (1200 RPM) until 260 RPS (15600 RPM).

Figure 3 shows the stiffness and damping coefficients for the cylindrical, elliptical and three-lobe hydrodynamic bearings, considering the value of preload equal to 0.

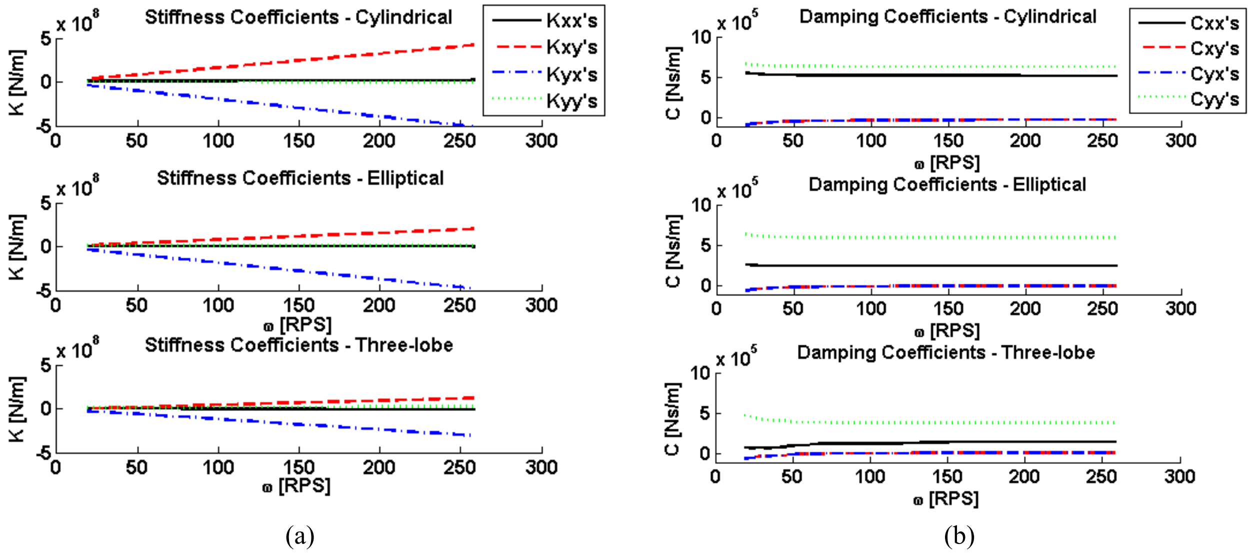

Figure 3. Equivalents coefficients of the cylindrical, elliptical and three-lobe hydrodynamic bearings, considering a null preload: (a) Stiffness coefficients, (b) Damping coefficients.

According to Fig. 3(a), it is possible to verify that the stiffness coefficients in multilobe bearings present the same behavior. These results show that the direct stiffness coefficients are approximately constant in the speed range analyzed. On the other hand, the cross-coupling stiffness coefficients tend to increase as the rotational speed increases. Moreover, the cylindrical bearing has the highest values of cross-coupled stiffness coefficients.

As occurred in the stiffness coefficients, the damping coefficients also have a similar behavior in the multilobe bearings, as verified in Fig. 3(b). Moreover, the damping coefficients are approximately constant in the speed range analyzed, being the direct damping coefficients higher than the cross-coupled damping coefficients. The differences in the coefficients magnitude in Fig. 3 (a) and (b) are due to the axial grooves in the multilobe bearings geometry, where the boundary conditions generally used are of null pressure in the lobes and pads ends.

Regarding the cross-coupling damping coefficients, due to the fact that they derive from self-adjoint operators, these coefficients are coincident. Therefore, the damping matrix will be symmetric and will have principal directions (with an orthonormal basis formed by eigenvectors). That is not true for the stiffness matrix where the cross-coupling stiffness coefficients are unequal, thus the stiffness matrix will be nonconservative (Lund, 1987).

Figure 4 shows the stiffness and damping coefficients for the elliptical, three-lobe and tilting pad journal bearings (LOB and LBP), considering the value of preload equal to 0.25.

As can be verified in Fig. 4(a), the direct stiffness coefficients in vertical direction (K_{yy}) have the highest value in the elliptical bearing. For the same reason, the damping coefficient in this direction increases as well, in Fig. 4(b). Regarding to the three-lobe bearing, although the cross-coupling stiffness coefficients are still higher, it is possible to verify an increasing tendency in the direct stiffness coefficients. The direct damping coefficients, however, remain higher than the cross-coupling damping coefficients.

The stiffness coefficients of the tilting pad journal bearing have similar behavior in both configurations (LOP or LBP). Nevertheless, differently from the multilobe bearings, the direct stiffness coefficients increases and the cross-coupling stiffness coefficients remain constant, as the rotational speed increases. In this case, direct stiffness coefficients are higher than the cross-coupling stiffness coefficients. Moreover, the damping coefficients are approximately constant in the range of speed analyzed, being the direct damping coefficients higher than the cross-coupling coefficients.

Figure 5 shows the stiffness and damping coefficients for the elliptical, three-lobe and tilting pad journal bearings (LOB and LBP), considering the preload of 0.5. In this case, the coefficients were plotted in different y-axis in order to facilitate the visualization and analysis.

The results presented in the Fig. 5 have a similar behavior presented in Fig. 4. However, it is possible to verify that the preload increasing tends to raise the direct stiffness and damping coefficients, mainly in multilobe bearings. Thus, the difference between the direct stiffness coefficient (K_{yy}) and the cross-coupling stiffness coefficient (K_{xy}) in the elliptical bearing is higher than in Fig. 4(a).

Moreover, the direct stiffness coefficients increase significantly in the three-lobe bearings. In both elliptical and three-lobe bearings, the damping coefficients have the same behavior presented in Fig. 4(b), increasing the magnitude due to the increasing of the preload.

Differently of the multilobe bearings, the stiffness coefficients in the tilting pad bearings do not increase significantly with the preload increasing, as verified in Figs. 4(a) and 5(a). On the other hand, the damping coefficients increasing due to the preload is expressive. Moreover, there is no significant difference between the coefficients obtained from the tilting pad journal bearings with configuration LOP or LBP.

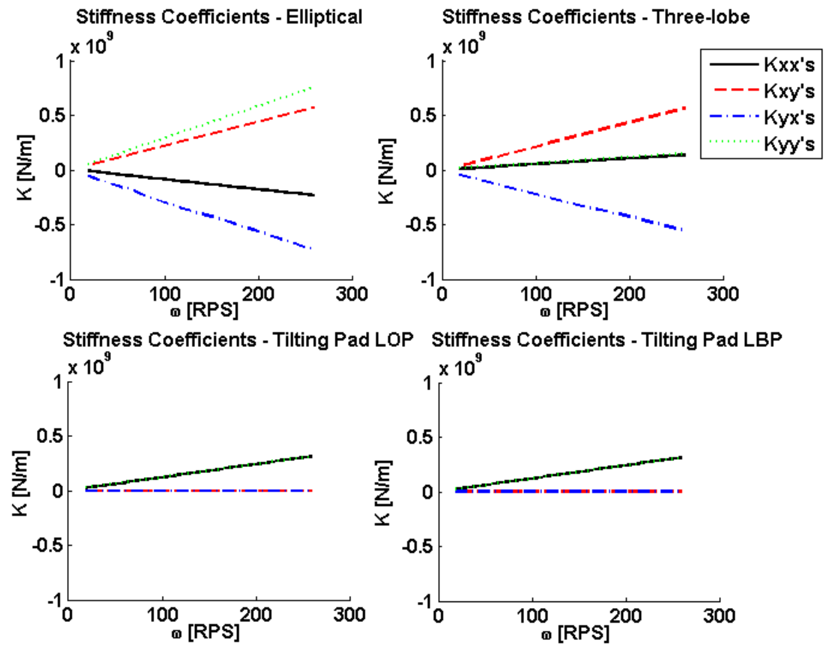

(a)

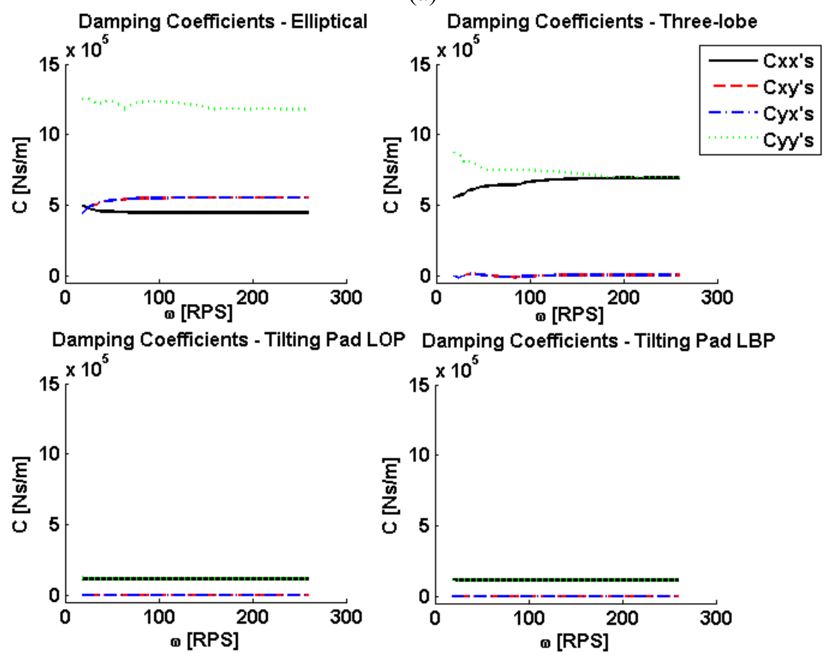

(b)

Figure 4. Equivalents coefficients of the elliptical, three-lobe and tilting pad journal bearings (LOB and LBP), considering the preload equal to 0.25. (a) Stiffness coefficients, (b) Damping coefficients.

Figure 6 shows the stiffness and damping coefficients for the elliptical, three-lobe and tilting pad journal bearings (LOB and LBP), considering the preload of 0.75. In this case, the coefficients were plotted in different y-axis in order to facilitate the visualization and analysis.

As already observed in the previous results (Figs. 4 and 5), the preload increasing tends to rise the direct stiffness and damping coefficients, mainly in the multilobe bearings. Because of that, although the behavior of the coefficients are the same, the magnitudes of the coefficients are higher in this case (Fig.6).

Differently of the previous cases, the direct stiffness coefficients (K_{xx} and K_{yy}) are higher than the cross-coupling stiffness coefficient (K_{xy} and K_{yx}) in the three-lobe bearing, as can be verified in the Fig. 6(a). It is important to highlight that the tilting-pad cross-coupled stiffness and damping coefficients are practically neglectable at high frequencies.

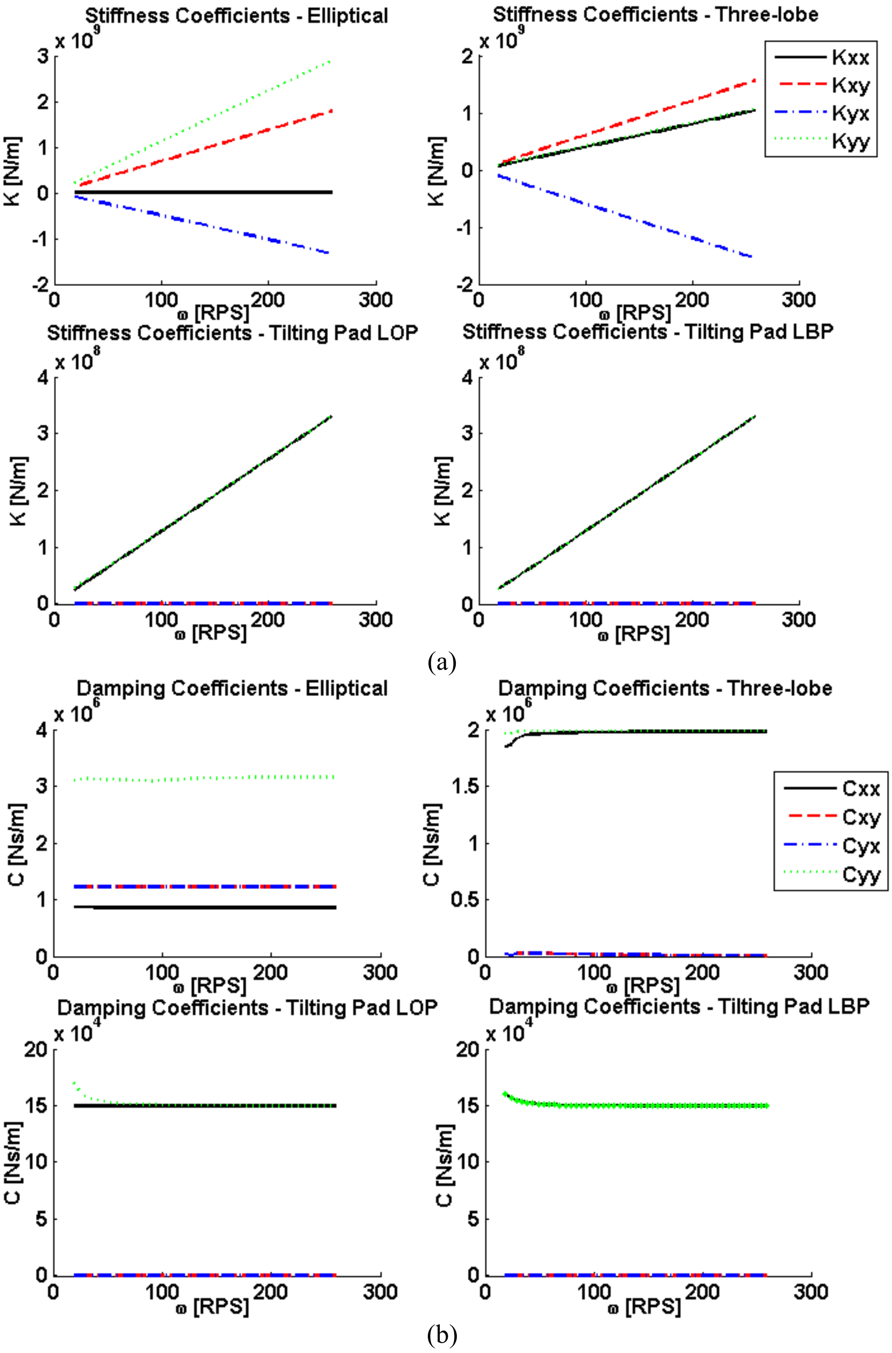

Figure 5. Equivalents coefficients of the elliptical, three-lobe and tilting pad journal bearings (LOB and LBP), considering the preload equal to 0.5. (a) Stiffness coefficients, (b) Damping coefficients.

According to Figs. 4 to 6, the tilting pad stiffness and damping coefficients do not present a significant difference when varying the preload from 0.25 to 0.75. The damping coefficients slightly change from preloads from 0.25 to 0.5. Besides, there are practically no changes to preloads from 0.5 from 0.75.

Figure 7 shows the locus of the shaft for cylindrical, elliptical, three-lobe and titling pad journal bearing (LOP and LBP), considering preloads of 0, 0.25, 0.5 and 0.75. In these figures, the dimensionless eccentricity and the attitude angle are shown in polar-coordinates graphs. The eccentricity was evaluated in a dimensionless form related to the radial clearance of the bearing. Hence, when the dimensionless eccentricity is 1, there is metal-metal contact between the shaft and the sleeve, and for a null eccentricity the shaft and the bearing are concentric.

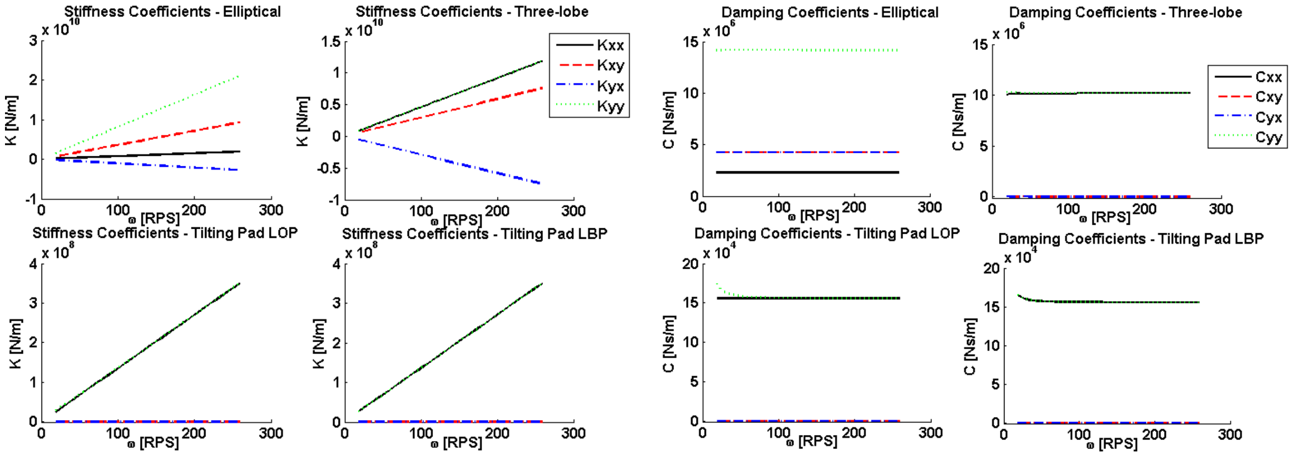

(a) (b)

Figure 6. Equivalents coefficients of the elliptical, three-lobe and tilting pad journal bearings (LOB and LBP), considering the preload equal to 0.75. (a) Stiffness coefficients, (b) Damping coefficients.

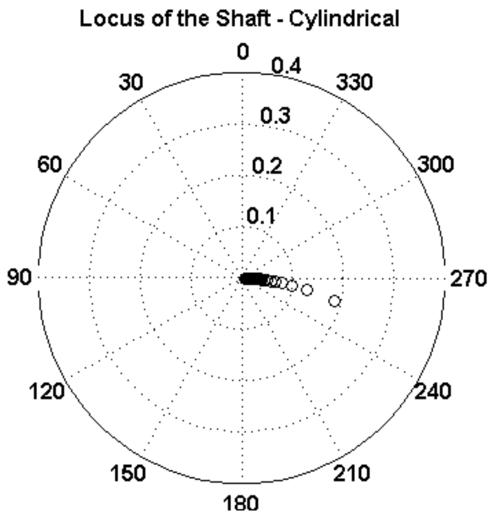

(a)

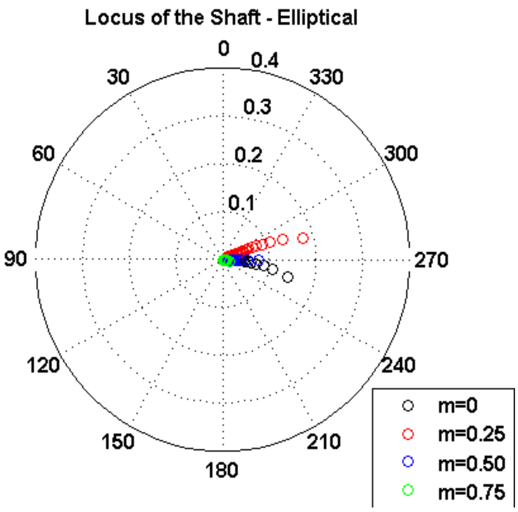

(b)

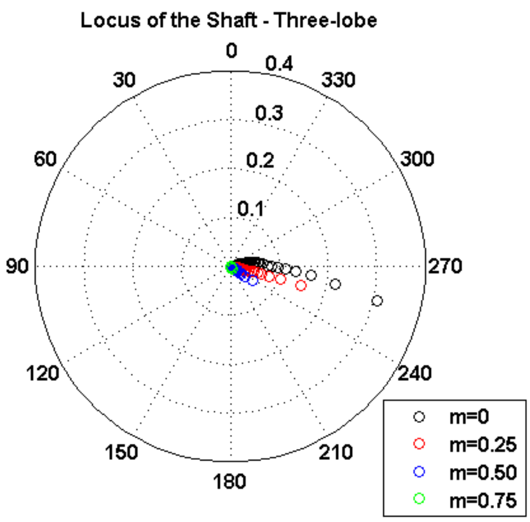

(c)

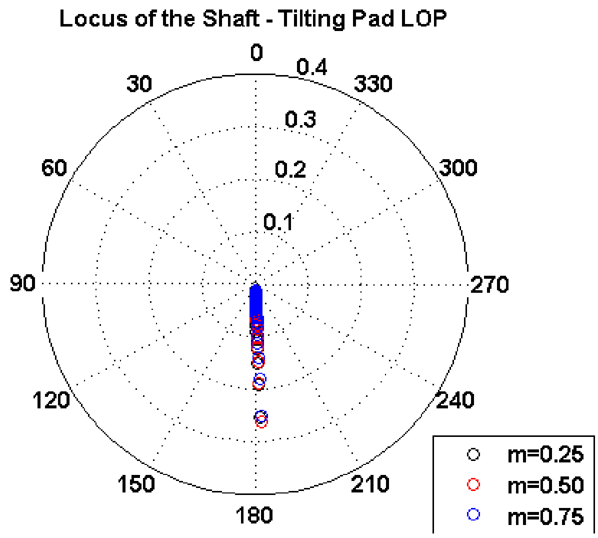

(d)

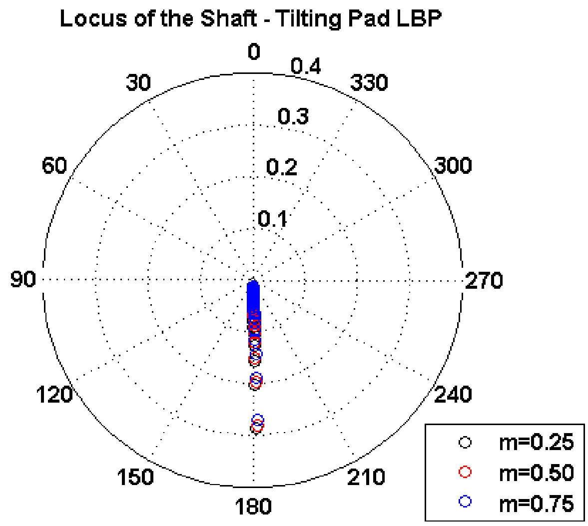

(e)

Figure 7. Locus of the Shaft. (a) Cylindrical , (b) Elliptical, (c) Three-lobe, (d) Tilting pad LOP, (d) Tilting pad LBP.

The variation of eccentricity and attitude angle occur with the change in the rotational speed. When the rotational speed of the shaft increases, the hydrodynamic forces in the bearing increase too. Thus, there is an increase of the attitude angle and a decrease in the eccentricity, causing the centralization tendency of the shaft inside the bearing at high rotation speeds. Due to operating conditions used in the simulations, the eccentricities in Figs. 7(a), 7(b) and 7(c) are small and, consequently, the attitude angles are high in the initial speed (20 RPS). Thus, it is possible to verify only a short displacement of the shaft in the bearing, which represents the final part of the characteristic curve obtained in the shaft locus.

Regarding the operating conditions, the load and rotational speed range were chosen so that the analysis of all bearings could be compared.

As verified in Fig. 7(a), the maximum dimensionless eccentricity of the shaft in the cylindrical bearing is about 0.2 (at 20 RPS) and the shaft goes to center of bearing as the rotational speed increases.

In the elliptical bearing with no preload, the behavior of the shaft is similar to that obtained in the cylindrical bearing. However, when considered a preload of 0.25, the shaft is located in the superior lobe of the bearing, because of the balance of the hydrodynamic forces (Machado and Cavalca, 2009). When considering a preload of 0.5 and 0.75, the shaft location is closer the center of bearing (lower dimensionless eccentricity), as can be verified in the Fig. 7(b).

According Fig. 7(c), the behavior of the shaft in the three-lobe bearing is similar to the cylindrical bearing. Moreover, it is possible to verify that the increasing of the preload tends to decrease the eccentricity ratio of the shaft.

Figures 7(d) and 7(e) show the locus of the shaft in the tilting pad bearing with configuration LOP and LBP, respectively. Differently from the results obtained in the multilobe bearings, the shaft tends to move vertically in the center line of the bearing, as the rotational speed increases. This behavior represents the better stability condition of the shaft in the bearing. Comparing Figs. 7(d) and 7(e), it is clear that the behavior of the shaft is similar in the tilting pad bearing with configuration LOP and LBP. Moreover, the eccentricity of the shaft decreases as the preload of the bearing increases.

4. CONCLUSIONS

From the analysis of the equivalent coefficients for cylindrical, elliptical, three-lobe and titling pad journal bearing (LOP-LBP), it is possible to verify that the damping and stiffness coefficients increase as the preload increases. However, the increasing of the stiffness coefficients in the tilting pad journal bearings (LOP and LBP) is very light.

Regarding stability in the hydrodynamic bearings, a qualitative analysis is made taking into account the relation among the direct and cross-coupling stiffness coefficients. Thus, at high rotational speed (small eccentricity), the bearing becomes more stable as higher is the direct stiffness coefficients compared to the cross-coupled stiffness coefficients, in a given direction (Gash at al, 2002).

In multilobe bearings with no preload, cross-coupling stiffness coefficients are higher than direct stiffness coefficients, showing that the cylindrical bearing does not present a good condition of stability in this case.

In elliptical bearing, as the preload increases, the direct stiffness coefficient (K_{yy}) becomes higher related to the cross-coupling stiffness coefficient (K_{xy}). Thus, the best condition of stability in elliptical bearing occurs with preload equal to 0.75, because in this situation there is the highest difference between the direct stiffness coefficient (K_{yy}) and the cross-coupling stiffness coefficient (K_{xy}).

A similar behavior is verified in the three-lobe bearing. In this case, a good condition of stability occurs because the direct stiffness coefficients increase in both directions, differently that in elliptical bearing.

The tilting pad journal bearings present good conditions of stability for all simulation of this paper, independent of the kind of configuration (LOP and LBP). In all simulations, the direct stiffness coefficients are higher than the cross-coupling stiffness coefficients in both directions. Actually, it can be observed that, in the cases studied here, the cross-coupled coefficients are practically neglectable at high frequencies compared to the direct ones

Finally, it is possible to verify that the application of tilting pad bearings results in better condition of stability in high rotational speed. However, this kind of bearing is more expensive than the multilobe hydrodynamic bearing. Because of that, the design of rotating machines in which the application of tilting pad bearings is unfeasible, the application of the preloaded multilobe bearings (elliptical or three-lobe) is recommend due to the improved condition of stability.

5. ACKNOWLEDGEMENTS

The authors thank CNPq, CAPES-PROBRAL programme and FAPESP for the financial support of this research.

6. REFERENCES

Allaire, P. E., Parsell, J. A., Barret, L. E., 1981, “A pad pertubation method for the dynamic coefficients of tilting pad journal bearing”. Wear, v. 72, p.29-44.

Bently, D. E., 2002, “Fundamentals of Rotating Machinery Diagnostics”, Bently Pressurized Bearing Press, Minden, NV, USA.

Castro, H. F.; Cavalca, K. L., 2008, “Whirl and whip instabilities in rotor-bearing system considering a nonlinear force model”, Journal of Sound and Vibration, v. 317, pp. 273-293.

Gunter, E. J.; Chen, W. J., 2005, “Introduction to Dynamics of Rotor-Bearing Systems”, Eigen Technologies, Inc, New York, NY, USA.

Lund, J. W., 1964, “Spring and Damping Coefficients for the Tilting-Pad Journal Bearing”, ASLE Trans, 7, pp. 342-352.

Lund, J. W., 1979, ‘‘Evaluation of Stiffness and Damping Coefficients for Fluid Bearings,’’ The Shock and Vibration Digest, Vol. 11, No. 1, pp. 5–10.

Lund, J. W., 1987, “Review of the Concept of Dynamic Coefficients for Fluid Film Journal Bearings”, ASME Journal of Tribology, vol. 109, pp. 37- 41.

Machado, T. H., Cavalca, K. L., 2009, “Evaluation of Dynamic Coefficients for Fluid Journal Bearings with Different Geometries”, In: 20th International Congress of Mechanical Engineering - COBEM 2009, Gramado-RS, Proceedings of the 20th International Congress of Mechanical Engineering. Rio de Janeiro : ABCM - Associação Brasileira de Ciências Mecânicas, v. 1. p. 1-11.

Maliska, C. R., 2004, "Transferência de Calor e Mecânica dos Fluidos Computacional", 2ª Ed, Livros Técnicos e Científicos Editora SA, Rio de Janeiro, RJ, Brasil.

Meruane, V.; Pascual, R., 2008, “Identification of nonlinear dynamic coefficients in plain journal bearings”, Tribology International, v. 41, pp. 743-754.

Ocvirk, F., 1952, “Short Bearing Approximation for Full Journal Bearing”, NACA TN 20808.

Pinkus, O., 1956, “Analysis of Elliptical Bearings”, Trans. ASME, v. 78, pp. 965-973.

Pinkus, O., 1958, “Solution of Reynolds Equation for Finite Journal Bearings”, Trans. ASME, v. 80, pp. 858-864.

Pinkus, O., 1959, “Analysis and Characteristics of Three-lobe Bearings”, Journal of Basic Engineering, pp. 49-55.

Reynolds, O., 1886, “On the Theory of Lubrication and its Application to Mr. Beauchamp Tower's Experiments, including an Experimental Determination of the Viscosity of Olive Oil”. Philosophical Transactions of Royal Society of London, Series A, Vol. 177, Part 1, pp.157-234.

Russo, F. H., 1999, Identificação das Propriedades Dinâmicas de Mancais Segmentados Híbridos – Teoria e Experimento, Dissertação de Mestrado, Faculdade de Engenharia Mecânica, Universidade Estadual de Campinas.

Sommerfeld, A., 1904, “Zur Hydrodynamischen Theorie der Schmiermittel-Reibung”, Zeitschrift für Math. Physik 40, pp. 97–155.

Wang, J. K.; Khonsari, M. M., 2006, “A new derivation for journal bearing stiffness and damping coefficients in polar coordinates”, Journal of Sound and Vibration, v. 290, pp. 500-507.

7. RESPONSIBILITY NOTICE

The authors are the only responsible for the printed material included in this paper.